

Exact solution and Majorana zero mode generation on a Kitaev chain composed out of noisy qubits

Marko J. Rančić*

TotalEnergies, Tour Coupole La Défense, 2 Pl. Jean Millier, 92078 Paris

(Dated: April 29, 2022)

Majorana zero modes were predicted to exist as edge states of a physical system called the Kitaev chain. Such zero modes should host particles that are their own antiparticles and could be used as a basis for a qubit that is to large extent immune to noise - the topological qubit. However, all attempts to prove their existence gave inconclusive results. Here, I experimentally show that Majorana zero modes do in fact exist on a Kitaev chain composed out of 3 noisy qubits on a publicly available quantum computer. The signature of Majorana zero modes is a degeneracy with the ground state which is not lifted by noise of the quantum computer. I also confirm that Majorana zero modes have a number of theoretically predicted features: a well-defined parity with switches at specific points and a non-conserved particle number. Furthermore, I show that Majorana zero modes favour long-range Majorana pairing at low chemical potential and short-range pairing at large values of the chemical potential. The results presented here are a most comprehensive set of validations ever conducted towards confirming the existence of Majorana zero modes in nature. I foresee that the findings presented here would allow any user with an internet connection to perform experiments with Majorana zero modes. Furthermore, the noisy intermediate scale quantum computing community can start building topological processors composed out of contemporary noisy qubits.

Introduction - A Majorana fermion is its own antiparticle. This concept originally proposed in the context of particle physics more than 80 years ago experienced a rebirth with the work of Alexei Kitaev in early 2000s [1]. Kitaev proposed a toy model composed out of a chain of spinless fermions which are coupled by tunnelling t in the presence of p -wave superconducting pairing Δ and tunable chemical potential μ . A Kitaev chain has an exceptional feature that at low chemical potential and when tunnelling is comparable to the superconducting pairing exact zero energy solutions localised at the edges exist. Such states are thought to be immune to any changes in local parameters and could potentially serve as a basis for a topological qubit.

Thus far, two considerable ways of solving the Kitaev Hamiltonian existed: numerical diagonalization of the many-body Hamiltonian and single-particle picture theories, such as diagonalizing the non-interacting Bogoliubov-de Gennes Hamiltonian. Numerical diagonalization of the many-body Hamiltonian is practically unfeasible for longer chains as the Hilbert space has 2^n states, where n is the number of sites in the chain. On the other hand, the Bogoliubov-de Gennes Hamiltonian operates on a Hilbert space of $2n$ states and has two zero energy solutions in the topological regime at low chemical potential. However, this Hamiltonian is a single-particle one and solves the Kitaev chain in a mean-field flavour.

Many theoretical proposals and experimental validations showing Majorana-like features followed after Kitaev's work [2–8]. Some of the works received broad attention from the scientific community such as the spin-orbit nanowire in the presence of an external magnetic field and proximitized superconductivity [9] and deposited iron atoms on top of a superconductor [10]. Nevertheless, most of these experimental validations were followed by theory or experiments of topologically trivial phenomena mimicking those of Majorana zero modes [11–17]. To date the existence of Majorana zero modes remained inconclusive.

Here, I will present a method of solving the Kitaev chain Hamiltonian exactly with a quantum computing methodology and prepare eigenstates of such a Hamiltonian in a topologically non-trivial regime on an actual quantum computer. The Kitaev chain in this study is composed out of noisy qubits. Given that there is no superconducting-non-superconducting state interface in this study, all topologically trivial explanations to the observed phenomena cannot be utilised.

Two eigenstates of a 3-site Kitaev chain will show a wide variety of features corroborating their Majorana zero mode nature: a robust to noise topological degeneracy with their ground states at low chemical potential and a well-defined parity. Furthermore, parity switches occur at points predicted by single-particle theories and the particle number of such states is not conserved. A finite Majorana-edge correlation function is indicative of long-range pairing and a Majorana site correlation function starts favouring pairing between neighbouring Majoranas as the chemical potential is increased.

* marko.rancic@totalenergies.com

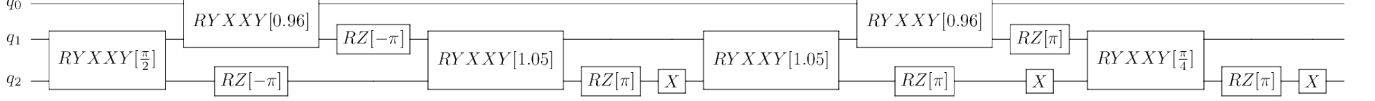


FIG. 1: The circuit which generates a ground state of a 3 site Kitaev Hamiltonian at $t = -1$, $\Delta = 1$ and $\mu = 10^{-8}$.

Methods - Throughout this paper I will display results obtained by executing code developed for a combination of IBM's Qiskit and Google's quantum AI Cirq. The key ingredient of the code is a method for exactly preparing eigenstates of quadratic Hamiltonians. Such states are called fermionic Gaussian states, as explained in Ref. [18] and are implemented with Google Quantum AI's Cirq OpenFermion [19]. Fermionic Gaussian states cannot describe excited states of exactly degenerate Hamiltonians [20]. Such wavefunctions are denoted as $|\psi\rangle$. As extensive numerical testing of the Kitaev chain showed multiple degeneracies at $\mu = 0$, I come as close to zero as $\mu = 10^{-8}|t|$.

The full n -site Kitaev chain Hamiltonian is given by

$$H = \sum_{k=1,n} \mu_k c_k^\dagger c_k - \sum_{\langle kj \rangle} (t_{kj} c_k^\dagger c_j - \Delta_{kj} c_k^\dagger c_j^\dagger + \text{H.c.}) . \quad (1)$$

Here, μ_k denotes the chemical potential at k th site, t_{kj} denotes the tunnel hopping between sites k and j , Δ_{kj} the superconducting pairing, c_k annihilates an electron at site k while c_k^\dagger creates the electron at the same site, and H.c. stands for an Hermitian conjugation. Majorana zero modes exist as solutions of the Kitaev Hamiltonian around $\mu = 0$ and $\Delta = -t$. This can be seen when substituting $c_k^\dagger = (\gamma_{2k-1} + i\gamma_{2k})/2$ and $c_k = (\gamma_{2k-1} - i\gamma_{2k})/2$ into Eq. (1), where γ_k is k th Majorana operator with the property $\gamma_k = \gamma_k^\dagger$. Throughout this paper, I will assume no local variations of these variables on different sites, hence μ_k , t_{kj} and Δ_{kj} become μ , t and Δ .

I will calculate and measure expectation values of a number of observables, the expectation value of energy $E = \langle \psi | H | \psi \rangle$, Majorana edge correlation function $\langle \psi | i\gamma_1 \gamma_{2n} | \psi \rangle$ [21] (where n denotes the number of sites and i denotes a complex number), Majorana site correlation function $\langle \psi | i\gamma_1 \gamma_k | \psi \rangle$, Majorana parity operator $\langle \mathcal{P} \rangle = \langle \psi | \prod_{k=1}^n (1 - 2c_k^\dagger c_k) | \psi \rangle$ and particle number operator $\langle N \rangle = \langle \psi | \sum_{k=1,n} c_k^\dagger c_k | \psi \rangle$. All of these quantities are expressed via fermionic creation and annihilation operators and transformed into a qubit representation via a Jordan-Wigner transformation [22].

According to Eq. (17) in Ref. [23], a topological state is supposed to exhibit parity switches at a chemical potential

$$\mu_{\text{PS}} = \pm 2\sqrt{t^2 - \Delta^2} \cos\left(\frac{\pi p}{n+1}\right), \quad (2)$$

where $p = 1, \dots, n/2$ for an even number of sites in the Kitaev chain n and $p = 1, \dots, (n-1)/2$ for an odd n .

In FIG. 1 I display a quantum computer circuit for generating a ground state of a 3-site Kitaev Hamiltonian at $t = -1$, $\Delta = 1$ and $\mu = 0^+ = 10^{-8}$, denoted by $[\cdot]$. This circuit is composed from nearest-neighbour two-qubit gates defined by $RYXXY(\alpha) = \exp(-i(X \otimes Y - Y \otimes X)\alpha/2)$, and $RZ(\beta)$ gates (rotations of the qubit around the z -axis of the Bloch sphere for an angle β) and X gate rotates a qubit around the x -axis of the Bloch sphere for an angle of π . All excited energy eigenstates of the 3-site Kitaev Hamiltonian at the given parameter regime are built by first applying X gates to appropriate qubits and then executing the circuit in FIG. 1. For instance the first excited state is obtained by applying an X gate to qubit q_0 followed by the execution of the circuit in FIG. 1 and is denoted as $[0]$. The highest energy state is obtained by applying X gates to qubits q_0, q_1, q_2 followed by the execution of the circuit in FIG. 1, and is denoted as $[0, 1, 2]$. Google Quantum AI's Cirq calculates the optimal angles α and β based on the input of μ , Δ and t .

Results - In FIG. 2 (a) I display the spectrum of a 3-site Kitaev chain Hamiltonian having $2^n = 8$ eigenstates. Here a comparison is given between a full diagonalization of the Kitaev Hamiltonian (black "x" symbols) and a solution obtained by implementing Gaussian states on an ideal quantum computer simulator (red and blue full lines). The red (blue) colour denotes states for which $\langle \mathcal{P}(\mu = 0^+) \rangle = +1(-1)$. Upon visual comparison these solutions show excellent agreement. The spectrum in subfigure (a) has a lowest energy state (highest energy state) with a next higher (lower) energy state degenerate to it around $\mu = 0$, and such degeneracies are marked with arrows.

In subfigure (b) I compare Gaussian states on an ideal simulator of quantum computers with their realisation on IBM Santiago. The circuit of the quantum eigenstate of the Kitaev chain is composed out of 6 two-qubit gates ($RYXXY$

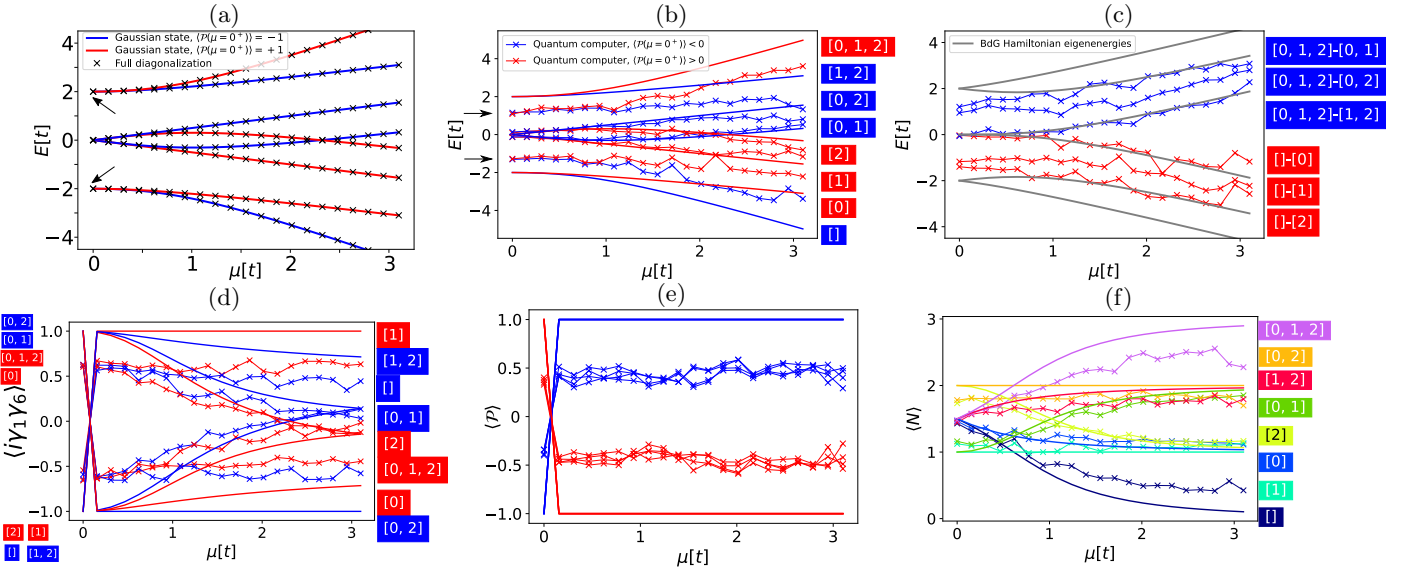


FIG. 2: Quantities of the Kitaev Hamiltonian at $t = -1$ and $\Delta = 1$ as a function of the chemical potential μ in units of absolute value of tunnelling $[t]$. (a-e) Black "x" symbols represent a result of a numerical diagonalization on a classical computer. Red "x" symbols (full lines) values obtained on a quantum computer (ideal simulator of quantum computers) with $\langle P(\mu = 0^+) \rangle = 1$. Blue "x" symbols (full lines) values obtained on a quantum computer (ideal simulator of quantum computers) with $\langle P(\mu = 0^+) \rangle = -1$. (a-b) The full spectrum of the Kitaev Hamiltonian obtained with Gaussian states compared to a numerical diagonalization (a) and IBM Santiago (b). The black arrows in (a-b) denote the position of the topological degeneracy. (c) The single-particle picture BdG spectrum (full line) compared to the BdG spectrum on IBM Santiago. (d) Majorana edge-correlation function, an ideal simulation compared to the actual 3-site Kitaev chain composed out of qubits. (e) Parity - an ideal simulation compared to the actual 3-site Kitaev chain composed out of qubits. (f) Particle number on an ideal simulator (full lines) and actual 3-site Kitaev chain composed out of qubits (x-shaped coloured symbols).

is implemented with two CNOT + single-qubit gates) and 9-13 single-qubit gates. The experiment is conducted for 8192 shots, with CNOT errors of 0.74% and readout errors of 1.5%. Single-qubit errors are not specified, however the average single-qubit frequency is 4.7 GHz with a pure dephasing time $T_2 = 70 \mu\text{s}$ and qubit relaxation time $T_1 = 83 \mu\text{s}$. Consequently, single-qubit gates influence the results much less than readout and two-qubit gate infidelity. Although all eigenstates move towards zero energy due to quantum noise, the degeneracy between states $[]$ and $[0]$ is not lifted by quantum noise. Similarly to that, the degeneracy between states $[1, 2]$ and $[0, 1, 2]$ follows the same pattern. This is an indication of their topological protection and the fact that states $[0]$ and $[1, 2]$ are indeed Majorana zero modes. In Supplementary Material S1 I give another realisation of the same experiment corroborating the existence of the topological degeneracy.

The BdG Hamiltonian solves the problem of the Kitaev chain in a single-particle picture. It features electrons and holes and their energy splitting from their ground state (that of electrons and that of holes). Even though the Kitaev chain is rather short, the BdG Hamiltonian (subfigure (c)) is indicating the presence of two zero energy eigenstates (zero in the context of how far away are they from their respective groundstate) which split in energy as the chemical potential μ is varied. This robust feature exist both in theory and on a noisy quantum computer. The BdG Hamiltonian has $2n = 6$ eigenstates for a 3-site Kitaev chain. States which are split from zero energy at low μ are often referred to as topologically trivial states in literature. It should be noted that although Majorana zero modes remained at zero energy, the topologically trivial states are further shifted towards zero as compared to theory due to quantum noise at low μ .

To further corroborate the Majorana zero mode nature of eigenstates of the Kitaev Hamiltonian I performed experiments and calculated the Majorana edge correlation function, $\langle i \gamma_1 \gamma_6 \rangle$, where 1 and 6 are indices of the Majoranas on the edge of the Kitaev chain. If this number is $+1(-1)$ this would mean that the Majoranas on the edges are correlated(anti-correlated) and if this number is 0 there is no Majorana pairing in the system. In subfigure (d) we see that the states $[0]$ and $[1, 2]$ behave exactly as predicted by mean-field theory, as the chemical potential is varied the Majorana states at the edges of the chain become less (anti)-correlated. However, the experimental value does not reach ± 1 due to quantum noise. For a more quantitative analysis of the measured data I revert the reader to Supplementary Material S2.

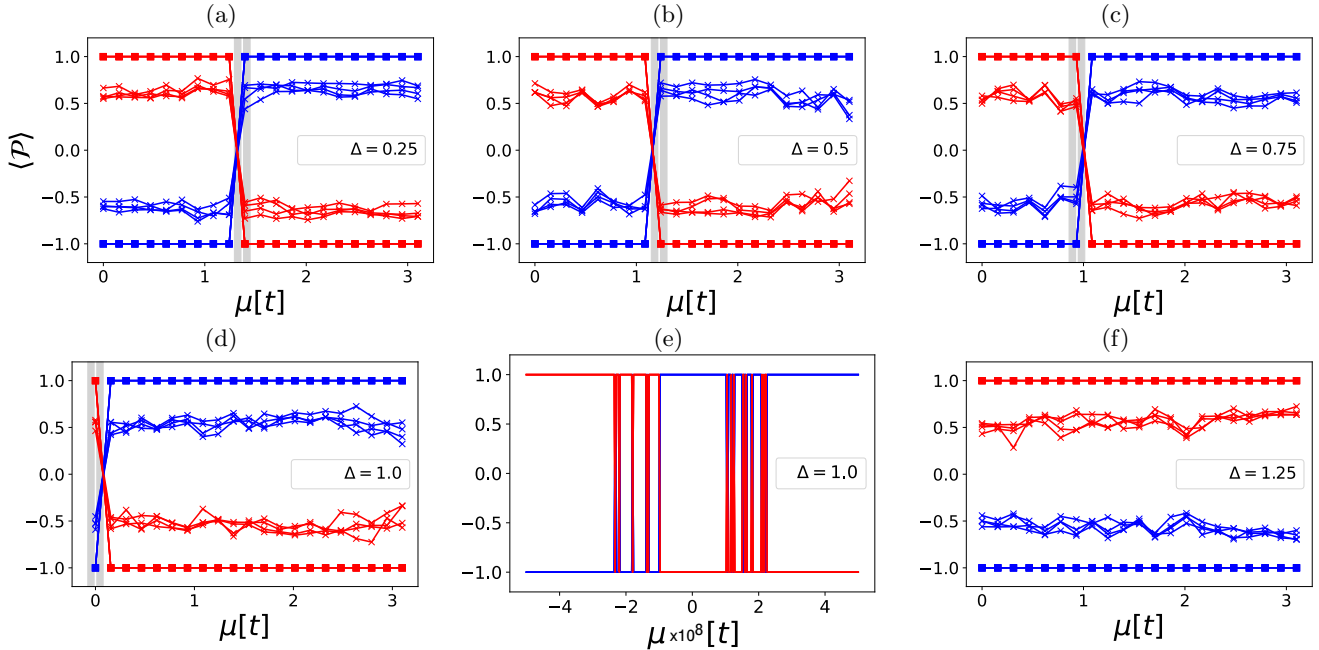


FIG. 3: (a-d) and (f) Parity switches at $t = -1$ for different values of Δ and for 20 values of μ between 10^{-8} and 3.1 with a 0.155 increment. (e) Parity switches for 400 values of μ between $-5 \cdot 10^{-8}$ to $5 \cdot 10^{-8}$.

As further consistency checks, I performed measurements and simulations of the parity of the eigenstates of the Kitaev Hamiltonian, and these results are displayed in subfigure (e). The eigenstates are clearly separated in terms of parity ± 1 in case of theory, and positive and negative in case of experiment. Similarly to energy measurements, the discrepancy between the theoretical and the experimental values is due to quantum noise. It should be noted that the eigenstates undergo a topological phase transition in which the parity of all eigenstates switches between the first two points ($\mu_1 = 10^{-8}$ and $\mu_2 = 0.155$). This topological phase transition is predicted to occur within the single-particle picture at $\mu = 0$ and will be discussed in detail later in this section.

Lastly in subfigure (f) I plot the total particle number of particles for different eigenstates. In general the Majorana zero modes are thought not to preserve particle number [24] and this is the case for states [0] and [1, 2].

In FIG. 3 I test the single-particle prediction that parity switches occur according to Eq. (2). Tunnelling is kept constant at $t = -1$, $\Delta = 0.25, 0.5, 0.75, 1, 1.25$ and μ is varied between 10^{-8} and 3.1 in 20 increments of 0.155. The points where parity switches represent a topological phase transition. Squared markers are added to ideal quantum simulator data. The grey line represents a region where the parity switching is likely to occur and it exists due to a limited resolution in μ in which the experiment is performed. The white line is the exact expected position of such a transition as predicted by the single-particle picture.

The results show that the behaviour of the exact solutions and the experiment is much in line with the prediction: parity switches occur exactly where they are predicted with Eq. (2). Here, I find the only minor discrepancy between the single-particle picture and the full solution - parity switches occur in a narrow parameter region in μ (see subfigure (e)) and not in a single point. However, this region in parameter space of μ is quite narrow - on the order of $4 \cdot 10^{-8}$ that I conclude that it is quite in line with predictions. A comparison between the simulated results (squares) and outputs of the quantum computers ("x" markers) show that this feature is quite robust to quantum noise. Although the value of the parity decreases on quantum computers as compared to ideal simulations, the point where parity switches is robust to any relaxation and pure dephasing. This is an indication that this parity switches represent a topological phase transition.

In FIG. 4 we observe the Majorana site correlation function $\langle i\gamma_1\gamma_k \rangle$ in the topological regime $\Delta = -t = 1$ as a function of the chemical potential μ . First it should be noted that the operator $i\gamma_1\gamma_k$ is non-Hermitian at $k = 1$ so the site correlation operator is an observable only when $k > 1$.

At low chemical potential states [0] and [1, 2] are exhibiting a Majorana-like character - a Majorana site correlation function localised at edges which is ± 1 for the results of an ideal simulation (full lines). The actual execution on a quantum computer (coloured "x" symbols) follows a similar qualitative trend but does not quantitatively reach ± 1 due to quantum noise. As the chemical potential increased, Majorana zero modes start favouring correlations between neighbouring Majorana fermions more. However, in the region of low μ , states [0, 2] and [1] have a robust long-range

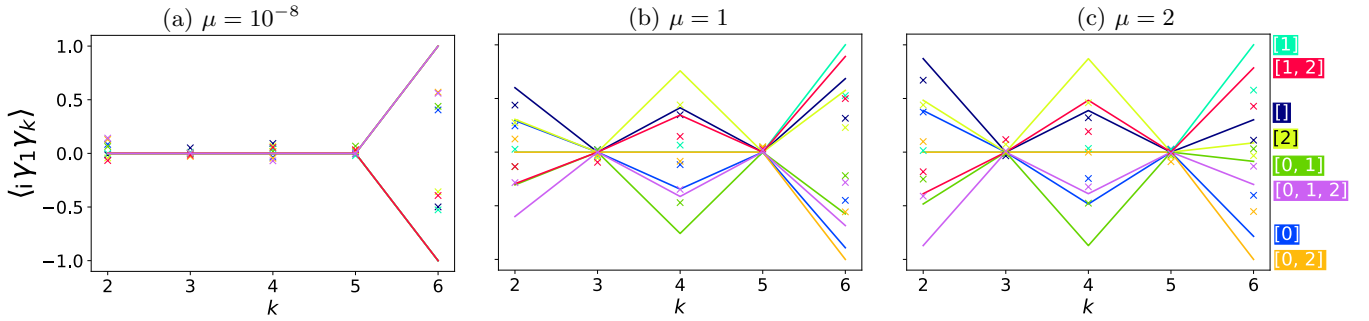


FIG. 4: Site correlation function where k denotes the site at different values of the chemical potential in the topological regime $\Delta = -t = 1$. Full lines denote values obtained by an ideal simulator of quantum computers at points of integer k and "x"-markers are output from IBM Santiago. Colour code is explained on the right.

correlation.

Conclusions - To conclude, here I solved the Kitaev chain exactly with quantum computing methods and showed both theoretically and experimentally that two eigenstates of the Kitaev Hamiltonian have a large number of features that corroborate their Majorana zero mode nature. They are zero energy excitations of their respective groundstate with a robust topological degeneracy, they have a Majorana edge-correlation function which decays with the chemical potential. Furthermore, Majorana zero modes favour Majorana pairing between edges of the Kitaev chain, do not preserve particle number and have parity switches at points in the parameter space as predicted by single-particle theories. The results presented here are the most complete set of experimental validations which confirm the existence of Majorana zero modes on the edges of a Kitaev chain.

Competing interest statement - The author declares no competing interests.

Acknowledgements - I would like to thank endlessly A. Lj. Rančić for all her patience, support and science discussions during the course of this work. I am also grateful to O. Dmytruk for live discussions and explanations.

-
- [1] A. Y. Kitaev, Physics-Uspekhi **44**, 131 (2001), URL <https://arxiv.org/abs/cond-mat/0010440>.
- [2] L. Fu and C. L. Kane, Phys. Rev. Lett. **100**, 096407 (2008), URL <https://link.aps.org/doi/10.1103/PhysRevLett.100.096407>.
- [3] L. Fu and C. L. Kane, Phys. Rev. B **79**, 161408 (2009), URL <https://link.aps.org/doi/10.1103/PhysRevB.79.161408>.
- [4] L. P. Rokhinson, X. Liu, and J. K. Furdyna, Nature Physics **8**, 795 (2012), URL <https://www.nature.com/articles/nphys2429>.
- [5] Q. L. He, L. Pan, A. L. Stern, E. C. Burks, X. Che, G. Yin, J. Wang, B. Lian, Q. Zhou, E. S. Choi, et al., Science **357**, 294 (2017), URL <https://science.sciencemag.org/content/357/6348/294>.
- [6] A. Banerjee, C. Bridges, J.-Q. Yan, A. Aczel, L. Li, M. Stone, G. Granroth, M. Lumsden, Y. Yiu, J. Knolle, et al., Nature Materials **15**, 733 (2016), URL <https://www.nature.com/articles/nmat4604>.
- [7] D. Wang, L. Kong, P. Fan, H. Chen, S. Zhu, W. Liu, L. Cao, Y. Sun, S. Du, J. Schneeloch, et al., Science **362**, 333 (2018), URL <https://science.sciencemag.org/content/362/6412/333>.
- [8] S. Manna, P. Wei, Y. Xie, K. T. Law, P. A. Lee, and J. S. Moodera, Proceedings of the National Academy of Sciences **117**, 8775 (2020), URL <https://www.pnas.org/content/117/16/8775>.
- [9] V. Mourik, K. Zuo, S. M. Frolov, S. Plissard, E. P. Bakkers, and L. P. Kouwenhoven, Science **336**, 1003 (2012), URL <https://science.sciencemag.org/content/336/6084/1003.abstract>.
- [10] S. Nadj-Perge, I. K. Drozdov, J. Li, H. Chen, S. Jeon, J. Seo, A. H. MacDonald, B. A. Bernevig, and A. Yazdani, Science **346**, 602 (2014), URL <https://science.sciencemag.org/content/346/6209/602>.
- [11] M. Ruby, B. W. Heinrich, Y. Peng, F. von Oppen, and K. J. Franke, Nano letters **17**, 4473 (2017).
- [12] J. D. Sau and P. M. R. Brydon, Phys. Rev. Lett. **115**, 127003 (2015), URL <https://link.aps.org/doi/10.1103/PhysRevLett.115.127003>.
- [13] E. J. Lee, X. Jiang, M. Houzet, R. Aguado, C. M. Lieber, and S. De Franceschi, Nature Nanotechnology **9**, 79 (2014), URL <https://www.nature.com/articles/nnano.2013.267>.
- [14] J. Chen, B. D. Woods, P. Yu, M. Hocevar, D. Car, S. R. Plissard, E. P. A. M. Bakkers, T. D. Stanescu, and S. M. Frolov, Phys. Rev. Lett. **123**, 107703 (2019), URL <https://link.aps.org/doi/10.1103/PhysRevLett.123.107703>.
- [15] B. D. Woods, J. Chen, S. M. Frolov, and T. D. Stanescu, Phys. Rev. B **100**, 125407 (2019), URL <https://link.aps.org/doi/10.1103/PhysRevB.100.125407>.
- [16] M. Kayyalha, D. Xiao, R. Zhang, J. Shin, J. Jiang, F. Wang, Y.-F. Zhao, R. Xiao, L. Zhang, K. M. Fijalkowski, et al., Science **367**, 64 (2020), URL <https://science.sciencemag.org/content/367/6473/64>.

- [17] H. Kim, Y. Nagai, L. Rózsa, D. Schreyer, and R. Wiesendanger, arXiv preprint arXiv:2105.01354 (2021), URL <https://arxiv.org/abs/2105.01354>.
- [18] Z. Jiang, K. J. Sung, K. Kechedzhi, V. N. Smelyanskiy, and S. Boixo, Phys. Rev. Applied **9**, 044036 (2018), URL <https://link.aps.org/doi/10.1103/PhysRevApplied.9.044036>.
- [19] J. R. McClean, N. C. Rubin, K. J. Sung, I. D. Kivlichan, X. Bonet-Monroig, Y. Cao, C. Dai, E. S. Fried, C. Gidney, B. Gimby, et al., Quantum Science and Technology **5**, 034014 (2020), URL <https://iopscience.iop.org/article/10.1088/2058-9565/ab8ebc>.
- [20] E. Greplova, *Quantum information with fermionic gaussian states* (2013).
- [21] J.-J. Miao, H.-K. Jin, F.-C. Zhang, and Y. Zhou, Scientific reports **8**, 1 (2018), URL <https://www.nature.com/articles/s41598-017-17699-y>.
- [22] A. Tranter, P. J. Love, F. Mintert, and P. V. Coveney, Journal of chemical theory and computation **14**, 5617 (2018), URL <https://pubs.acs.org/doi/10.1021/acs.jctc.8b00450>.
- [23] S. Hegde, V. Shivamoggi, S. Vishveshwara, and D. Sen, New Journal of Physics **17**, 053036 (2015), URL <https://iopscience.iop.org/article/10.1088/1367-2630/17/5/053036/meta>.
- [24] Y. Lin and A. J. Leggett, arXiv preprint arXiv:1803.08003 (2018), URL <https://arxiv.org/pdf/1803.08003.pdf>.

Supplementary Material: Exact solution and Majorana zero mode generation on a Kitaev chain composed out of noisy qubits

S1. COMPARISON BETWEEN RUNS OF HARDWARE

In this section I compare two different experiment runs on IBM Santiago in FIG. S1. Although the different executions vary slightly quantitatively depending on the calibration of the device all qualitative features remain present, especially the topological degeneracy.

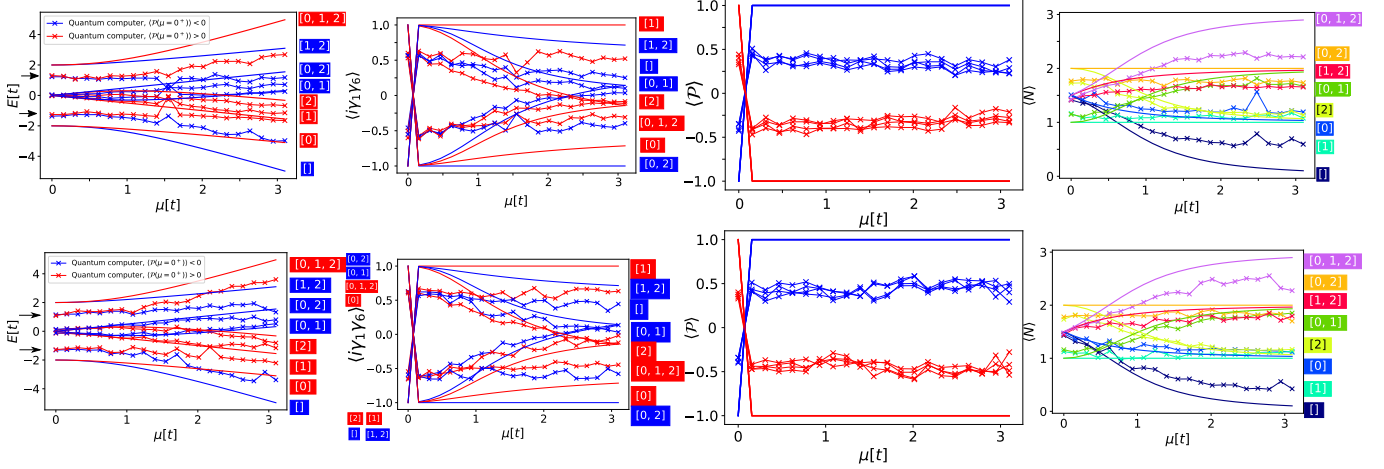


FIG. S1: TOP - first realisation of: Energy, Majorana edge correlation function, parity and particle number respectively as a function of chemical potential. BOTTOM - second realisation (main body of paper) of: Energy, Majorana edge correlation function, parity and particle number respectively as a function of chemical potential. Full lines denote ideal simulation, x-points connected with lines are a result of an experiment on IBM Santiago.

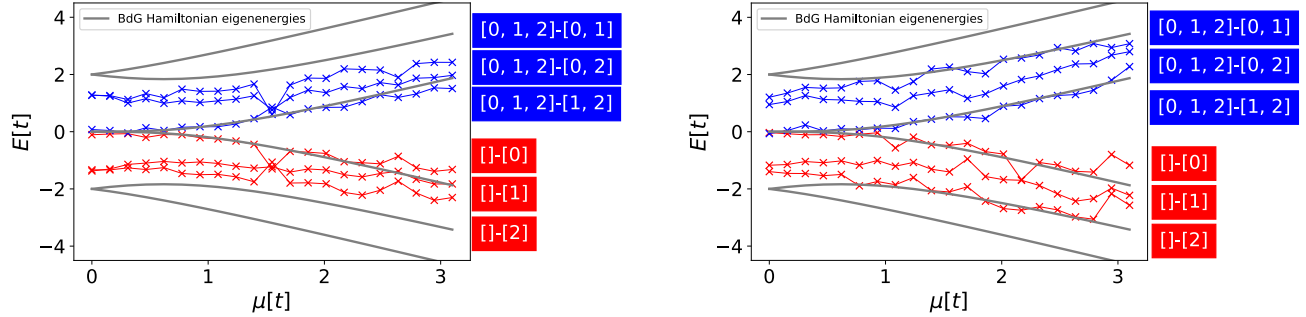


FIG. S2: The BdG Hamiltonian theory (grey) and experiment (blue and red). Left: first realisation of the experiment, right: second realisation of the experiment (main body of the paper).

S2. THE MAJORANA EDGE CORRELATION FUNCTION

In the thermodynamic limit, the Majorana edge correlation function is expected to decay with a quadratic dependence in μ [S21]. As comparing a $n = 3$ site Kitaev chain with a theory developed for an infinitely long chain is infeasible, I will just give mean square fits of the decay of the absolute value of the Majorana edge correlation function $|\langle i\gamma_1\gamma_k \rangle|$, with a goal of outlining the fact that Majorana edge correlations do indeed decay as a function of μ . The polynomial fit to data for the first run (left) for state $[0]$ is $0.57 - 0.18\mu + 0.03\mu^2$ and for the state $[1, 2]$ is $0.56 - 0.18\mu + 0.03\mu^2$ with respective residuals 0.03 and 0.02. The polynomial fit to data for the second run (right, main body of the paper) for state $[0]$ is $0.63 - 0.14\mu + 0.03\mu^2$ and for state $[1, 2]$ $0.6 - 0.09\mu + 0.01\mu^2$ with residuals of 0.01 and 0.03 respectively. The device was calibrated between runs.

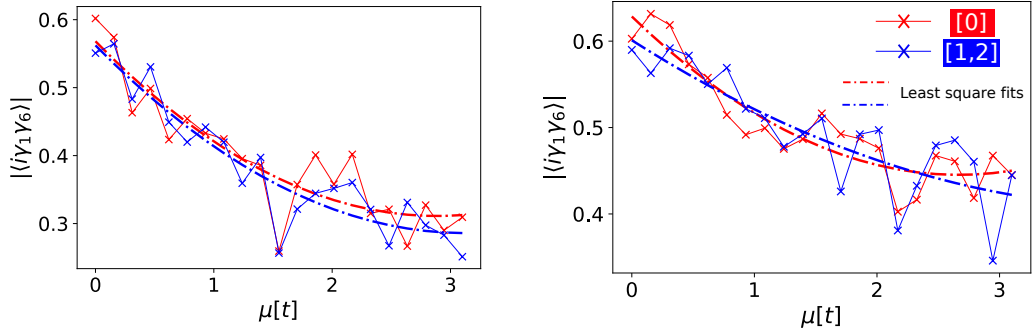


FIG. S3: The absolute value of the correlation function of Majorana zero modes. Left: first realisation of the experiment, right: second realization of the experiment (main body of the paper).

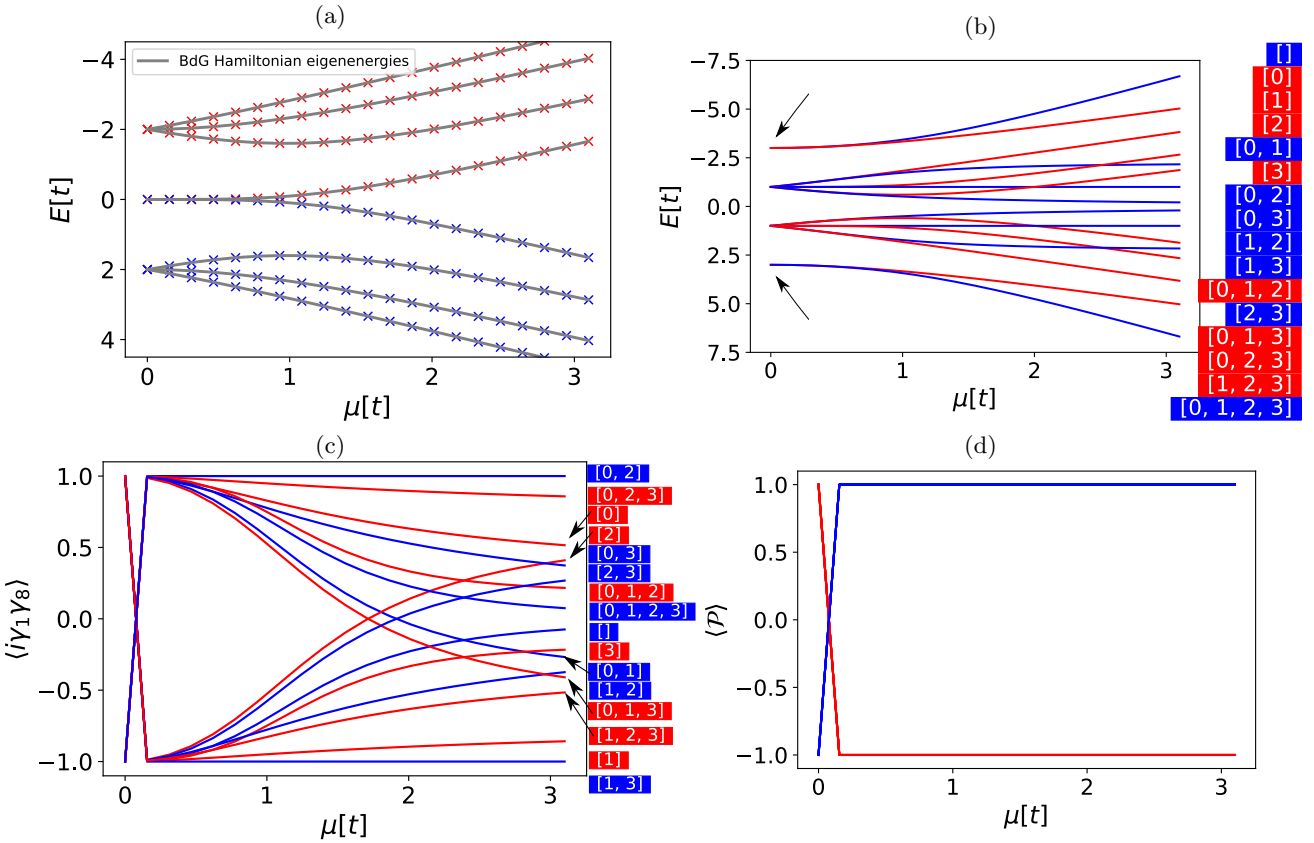


FIG. S4: Quantities of a 4-site Kitaev Hamiltonian at $t = -1$ and $\Delta = 1$ as a function of the chemical potential μ in units of absolute value of tunnelling $[t]$. Red denotes values obtained on an ideal simulator of quantum computers with $\langle P(\mu = 0^+) \rangle = 1$. Blue denotes values obtained on an ideal simulator of quantum computers with $\langle P(\mu = 0^+) \rangle = -1$. (a) The single-particle picture BdG spectrum, diagonalization of the BdG Hamiltonian (grey lines) compared to Gaussian state solutions (coloured markers). (b) The full spectrum computed by Gaussian states. Black arrows indicate the topological degeneracy. (c) Majorana edge-correlation function, an ideal simulation with fermionic Gaussian states implemented on a quantum computing simulator. (d) Parity - an ideal simulation with Gaussian states.

S3. A 4-SITE KITAEV CHAIN

The formalism presented here allows the treatment of longer Kitaev chains with quantum simulators. Actual quantum computing preparation of Kitaev states should somewhat still be possible with currently available quantum computing hardware, however the author of this paper has no access to state of the art quantum computers and I

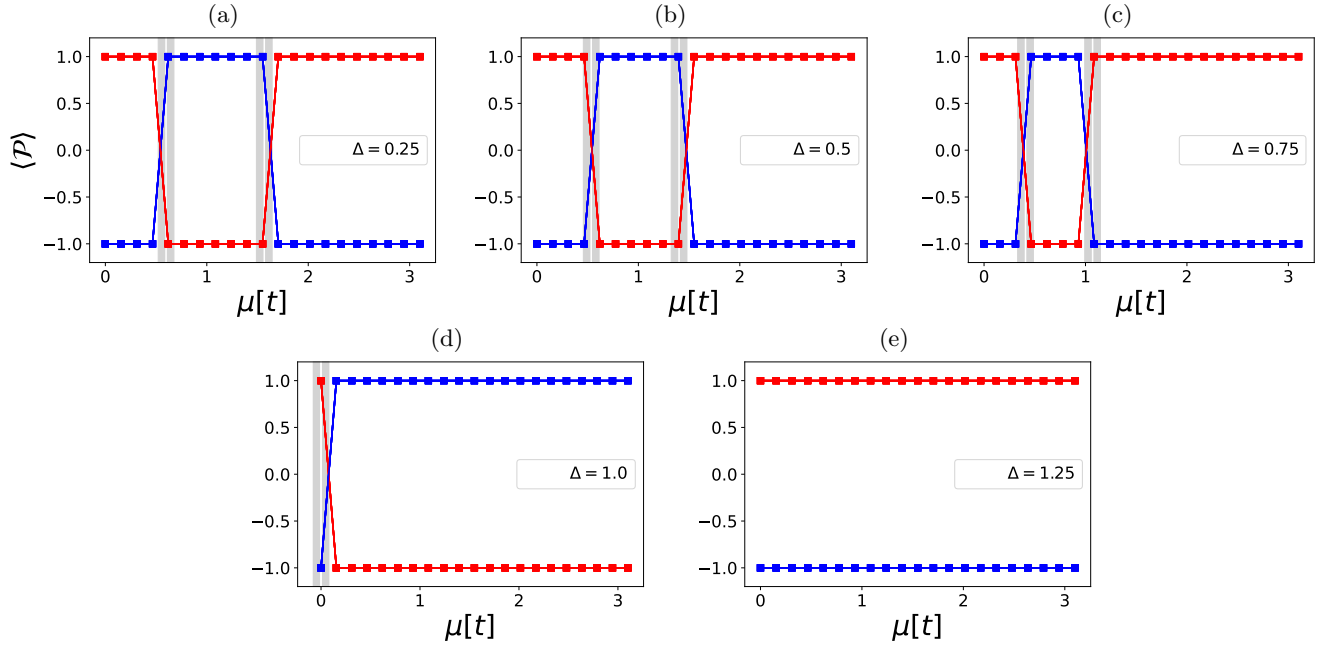


FIG. S5: (a-e) Parity switches at $t = -1$ for different values of Δ and for 20 values of μ between 10^{-8} and 3.1 with a 0.155 increment for an $n = 4$ Kitaev chain. White lines are predictions of Eq. (2) and grey areas are the regions in which parity switches potentially exist due to finite resolution in μ .

will thus only focus on results from quantum simulators in the remainder of this supplementary material.

In FIG. S4 I compare results obtained by an ideal simulation of Gaussian states with BdG energies (a) and display the eigenspectrum obtained on a quantum computing simulator (b).

In subfigure (c) Majorana edge-correlation functions are shown with states $[0]$ and $[1, 2, 3]$ having a decay of the edge correlation function. Parity switches are also in accordance with single-particle picture theories. In FIG. S5 I show a matching between parity switches predicted by Gaussian states implemented on an ideal quantum computing simulator and white lines are predictions of Eq. (2). Grey areas are ranges in parameter space of μ where parity switching exists due to a finite resolution of μ .

Also in similarity with the 3-site case Majorana zero modes start favouring pairing between neighbouring Majoranas as the chemical potential is increased see states $[0, 2, 3]$ and $[1]$ in FIG. S6.

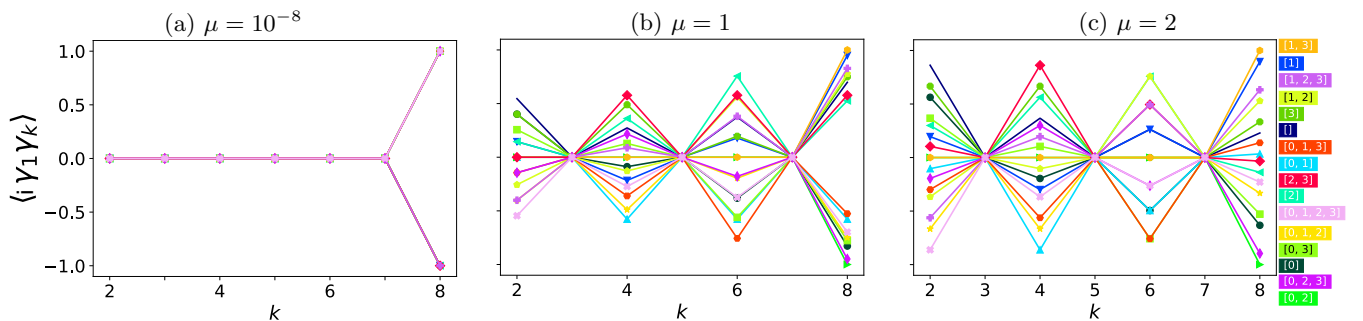


FIG. S6: Site correlation function where k denotes the site at different values of the chemical potential in the topological regime $\Delta = -t = 1$ obtained by fermionic Gaussian states. The colour code is explained on the right.